# REMARKS

## FORMAL MATTERS:

Claims 1-24 are pending after entry of the amendments set forth herein.

Claims 1 and 4-24 were withdrawn from consideration as follows:

- Claims 1 and 13-16 are withdrawn from consideration, but are linking claims to be addressed after the elected subject matter is deemed allowable.
- Claims 4-12 and 17-24 are withdrawn as being drawn to a non-elected invention, the restriction requirement being made final.

Claim 3 is amended for clarity.

No new matter is added.

## RESTRICTION REQUIREMENT - FINAL

Applicants acknowledge that the Restriction Requirement has been made final, and expressly reserve the right to petition for review of same. All claims of the non-elected groups have been maintained as pending.

## TREATMENT OF LINKING CLAIMS

The Office Action indicates that claims 1 and 13-16 are linking claims, but at the same time are withdrawn from consideration and will be addressed after the elected subject matter is deemed allowable.

According to MPEP §809, the linking claims must be examined with the invention elected, and should any linking claim be allowed, the restriction requirement must be withdrawn. Any claim(s) directed to the nonelected invention(s), previously withdrawn from consideration, which depends from or includes all the limitations of the allowable linking claim must be rejoined and will be fully examined for patentability. Where such withdrawn claims have been canceled by applicant pursuant to the restriction requirement, upon the allowance of the linking claim(s), the examiner must notify applicant that any canceled, nonelected claim(s) which depends from or includes all the limitations of the allowable linking claim may be reinstated by submitting the claim(s) in an amendment. Upon entry of the amendment, the amended claim(s) will be fully examined for patentability

Consideration of linking claims 1 and 13-16 on the merits is thus respectfully requested.

**REJECTIONS UNDER §112, ¶2**

Claim 3 was rejected as being indefinite. Each aspect of this rejection is addressed below

***"binding to a surface structurally defined by . . . residues 342 and 349"***

The Office has rejected claim 3 for recitation of the above phrase on the grounds that it is not clear "under which conditions the residues (that are flexible) identify a flat surface; furthermore, which part of the residues serve as 'identifier' for the surface."

First, Applicants respectfully submit that there is no requirement in the claim that the surface defined by these residues be "flat".

Second, reference to a "surface structurally defined by poliovirus RNA-dependent RNA polymerase residues 342 and 349 or residues at corresponding positions in a RNA-dependent RNA polymerase" in claim 3 is meant to refer to a particular portion of Interface I of an RNA-dependent RNA polymerase, using the amino acid sequence of poliovirus RNA-dependent RNA polymerase as a reference point. Figure 2C shows the structure of Interface I in poliovirus RNA-dependent RNA polymerase, including the position of residues 342 and 349.

***"surface defined by . . . corresponding positions thereof"***

The Office has rejected claim 3 for recitation of "surface identify by . . . corresponding positions thereof" on the grounds that "corresponding positions thereof" is not defined.

Applicants respectfully note that the phrase "corresponding positions" is indeed defined in the specification at paragraph [0043] to mean:

> the position of an amino acid in a peptide . . . corresponds to the same position in the sequence of the conserved binding surface of different viral polymerases, i.e. different but related positive strand virus such as a picornavirus and a flavivirus. Thus a residue in a specific position in Interface I of a poliovirus will have a "corresponding position" in the conserved interface of a different picornavirus, a flavivirus, etc.

***binding of pharmacophore***

The Office further rejected claim 3 on the grounds that it is not clear "whether the pharmacophore is supposed to bind the indicated . . . residues themselves, or the surface defined thereby."

Applicants respectfully submit that this distinction drawn by the Office is not understood. As noted above, a "surface structurally defined by poliovirus RNA-dependent RNA polymerase residues 342 and 349 or residues at corresponding positions in a RNA-dependent RNA polymerase" in claim 3 is meant to refer to a particular portion of Interface I of an RNA-dependent RNA polymerase, using the amino acid sequence of poliovirus RNA-dependent RNA polymerase as a reference point.

***Conclusion***

Withdrawal of the rejections of claim 3 under §112, ¶2 is respectfully requested.

**REJECTIONS UNDER §112, ¶1 – "WRITTEN DESCRIPTION"**

Claims 2 and 3 were rejected under §112, ¶1 on the grounds that the claims contain subject matter not adequately described in the specification. The Office Action states that

> The claims are drawn to a pharmacophore that binds to surface defined by residues 342 and 349 of RNA-polymerase. Specification does not describe any pharmacophore that binds, specifically, to said residues of RNA-polymerase. Example 10 (pages 47-49) does describe peptide SEQ ID No. 5 which does disrupt RNA-polymerase functions. However, there is no evidence that said polypeptide belongs to the genus as claimed, i.e, that it does bind to the specified residues 342 and 349 of RNA-polymerase.

(Office Action, page 4)

This rejection is respectfully traversed.

As described in the specification (see, e.g., paragraph [00105]), Interface I interactions involve 21 direct amino acid side chain interactions, at least 5 water mediated interactions and one direct backbone-backbone hydrogen bond. The interactions at Interface I can be divided into two distinct regions. The first region (at the top of Interface I in Figure 2C) centers around L446 which extends from the surface of one polymerase molecule and into a hydrophobic pocket in the adjacent polymerase molecule. The hydrophobic pocket of this second molecule is formed from two separate peptide loops which immediately precede and follow the conserved poliovirus polymerase C motif. Numerous direct

as well as water mediated interactions also occur between the residues in these two loops and the residues flanking L446.

The second region of interaction at Interface I involves two α -helices (the C-terminal α-helix of one molecule and the motif D α -helix of the second molecule) that pack together at an angle of approximately 90°. Almost all of the surface exposed amino acid side chains on both of these helices interact across this interface. These interactions include R455 from one helix which hydrogen bonds with D349 from the helix of the adjacent polymerase molecule as well as L342 from one molecule, which packs against a hydrophobic patch on the other polerase molecule.

Applicants submit that the inhibitor peptide is reasonably expected to interact with the portion of Interface I having the residues 342 and 349 because the inhibitor is designed based on the sequence of the alpha-helix that interacts with this region in the polymerase. The peptide described in the application as exemplary of pharmacophores that disrupt polymerase binding at Interface I -- KPHKCTFEGCRKSYSRSTNLRRHLNSH (SEQ ID NO:5) –was designed to mimic the continuous α-helix at Interface I. See, Example 10, paragraphs [00156] – [00164], particularly paragraph [00158]. In other words, the α-helix this peptide was designed to mimic an amino acid sequence present in the polymerase subunit that interacts with the region of Interface I having residues 342 and 349. Thus the peptide of SEQ ID NO:5 does indeed provide an example of a pharmacophore of the present claims.

Once provided with the knowledge of the three-dimensional structure of RNA-dependent RNA polymerase, and further when provided with the inventors' discovery that a peptide designed to mimic the α-helix at Interface I can inhibit polymerase function, the ordinarily skilled artisan can design additional inhibitors using this information.

Withdrawal of this rejection is respectfully requested.

**REJECTIONS UNDER §112, ¶1 – "ENABLEMENT"**

Claims 2 and 3 were rejected under §112, ¶1 on the grounds that the specification is not enabling for making of the product as claimed. This rejection is respectfully traversed

As Applicants understand it, this rejection flows from the rejection of the claims under §112, ¶2. Specifically, the rejection is based on the assertion that the claim language means that the pharmacophore binds not particular residues of RNA polymerase, but rather binds a surface "defined by" the residues.

This rejection arises since the Office has taken the position that the term "surface structurally defined by . . . residues 342 and 349" is not clear. Based on this, the Office asserts that it is not clear how to make products that satisfy the claimed structural limitations. Further, the Office asserts that although the specification reviews known methods of drug modeling, this description does not address the issue of undefined structure to which the pharmacophore is to bind. The Office again asserts that there is no evidence the peptide of SEQ IDNO:5 – which does disrupt RNA-polymerase function – binds to the specified residues 342 and 349 of RNA-polymerase.

Applicants respectfully submit that this rejection is addressed in view of the clarification to the claims as described above in the context of the rejections under §112, ¶2. For example, reference to a "surface structurally defined by poliovirus RNA-dependent RNA polymerase residues 342 and 349 or residues at corresponding positions in a RNA-dependent RNA polymerase" in claim 3 is meant to refer to a particular portion of Interface I of an RNA-dependent RNA polymerase, using the amino acid sequence of poliovirus RNA-dependent RNA polymerase as a reference point. Figure 2C shows the structure of Interface I in poliovirus RNA-dependent RNA polymerase, including the position of residues 342 and 349.

As to the binding of the peptide of SEQ ID NO:5 to this region of Interface I, this has been addressed above in the context of the written description rejection under §112, ¶1. In short, the peptide of SEQ ID NO:5 was designed to mimic mimic an amino acid sequence present in the polymerase subunit that interacts with the region of Interface I having residues 342 and 349. Thus the peptide of SEQ ID NO:5 does indeed provide an example of a pharmacophore of the present claims.

There is ample information available regarding the structure of Interface I in poliovirus RNA-dependent RNA polymerase, as well as the structure of Interface I among other viral RNA-dependent RNA polymerases in view of its conserved nature across viruses. Methods of molecular modeling for production of pharmacophores that interact with a structure of interest are also known. Thus, once provided with the inventors' discovery that, for example, disruption of RNA-dependent RNA polymerase interactions at Interface I, e.g., by binding of a pharmacophore at this site, inhibits polymerase activity, the ordinarily skilled artisan can readily make such compounds.

Withdrawal of this rejection is respectfully requested.

**REJECTIONS UNDER §102**

Claims 2 and 3 are rejected as anticipated by Sergio et al. (US 6,492,423). This rejection is respectfully traversed.

Sergio et al. is cited for its disclosure of diketoacids that inhibit viral polymerases, particular RNA-dependent RNA polymerase. The rejection is based on the Office's position that since these diketoacids inhibit RNA-dependent RNA-polymerase, the are inherently capable of binding to the RNA-dependent RNA-polymerase. The Office assumes that, in the absence of evidence to the contrary, the inhibitors of Sergio et al. bind to the RNA-dependent RNA-polymerase in the manner required by the instant claims, and shifts the burden to Applicants to show a novel or unobvious difference between the claimed product and that of Sergio et al.

The pharmacophores of the current claims are designed to disrupt interactions at Interface I, particularly at the region defined by residues 342 and 349.

In contrast, the Sergio et al patent is for a group of compounds that target the active sites of RNA-dependent RNA polymerases. Specifically, Sergio et al. col. 1, lines 30-41 states:

> DISCLOSURE OF THE INVENTION
>
> The present inventors have discovered that a range of diketoacids have utility as enzyme inhibitors and, in particular, as polymerase inhibitors and more particularly as inhibitors of hepatitis C NS5 RNA-dependent RNA polymerase, HBV DNA-dependent RNA polymerase and HIV DNA-dependent DNA polymerase. Their investigations indicate that these compounds may act by interfering with the binding of phosporyl groups at the active site of the enzyme and may, therefore, have broad application in inhibiting enzymes involved in the transfer of phosphoryl groups.

Sergio et al. describes several compounds of different formulas that fall within the diketoacid class. Also at col. 89, line 61- 90, Sergio et al. states:

> While not wishing to be bound by any particular theory, the present inventors hypothesize that the diketoacid fragment of the compounds of the present invention inhibits RNA dependent polymerase activity by providing an "active site anchor" and interacting with divalent metal cations ($Mg^{2+}$, $Mn^{2+}$) required for polymerase activity. The ring system found on the left hand side of the molecule can
>
> apparently be modified in order to build specificity towards a giver polymerase.

The crystal structure of RNA-dependent RNA polymerase shows that the binding surfaces at Interface I (as well as the binding surfaces at Interface II) are distinct from the active site targeted by Sergio et al. See, e.g., Lyle et al. (2002) *Science* 296:2218-2222 (copy attached).

Therefore, the inhibitors of Sergio et al. are not inhibitors of the claimed invention, as they are not pharmacophores that interact with Interface I of a viral RNA-dependent RNA polymerase, e, g., by binding to a surface structurally defined by poliovirus RNA-dependent RNA polymerase residues 342 and 349.

Withdrawal of this rejection is thus respectfully requested.

**CONCLUSION**

Applicant submits that all of the claims are in condition for allowance, which action is requested. If the Examiner finds that a telephone conference would expedite the prosecution of this application, please telephone the undersigned at the number provided.

The Commissioner is hereby authorized to charge any underpayment of fees associated with this communication, including any necessary fees for extensions of time, or credit any overpayment to Deposit Account No. 50-0815, order number STAN-193.

Respectfully submitted,
BOZICEVIC, FIELD & FRANCIS LLP

Date: June 21, 2004

By: _____
Carol L. Francis
Registration No. 36,513

BOZICEVIC, FIELD & FRANCIS LLP
200 Middlefield Road, Suite 200
Menlo Park, CA 94025
Telephone: (650) 327-3400
Facsimile: (650) 327-3231

Enclosure: Lyle et al. (2002) *Science* 296:2218-2222

F:\DOCUMENT\STAN (Stanford)\193\Amendment in resp to oa 3.22.04.doc

into the ER lumen (Fig. 3C). Glycosylation of $Asn^{10}$ and $Asn^{20}$ was also confirmed in vitro (*13*).

On the basis of the analysis of glycosylation sites and the prediction of transmembrane regions, we propose a seven-transmembrane topology for SPP with the $NH_2$-terminus in the ER lumen, the COOH-terminus containing the ER retrieval signal in the cytosol, and the active-site motifs YD and LGLGD in the center of adjacent transmembrane regions (Fig. 3D). Such motifs are also present in adjacent transmembrane regions of presenilins (*3*, *5*, *6*). However, the predicted orientation of the transmembrane regions containing the YD and LGLGD motifs is opposite in presenilins compared with that of SPP, in accordance with the opposite orientation of the substrates. The substrates of presenilins, NOTCH-1 and β-APP, are type I membrane proteins, whereas SPP substrates have a type II orientation (Fig. 3D).

Genetic evidence supports the explanation that presenilins are γ-secretases, which catalyze cleavage of β-APP in its transmembrane region and liberate Aβ peptides (*6*). Recent observations, however, question presenilins as the proteolytic components that cleave β-APP and NOTCH and suggest alternative functions, such as that of a molecular chaperone for membrane proteins (*20*). The identification of SPP as a presenilin-type aspartic protease favors the former view that presenilins are proteases. The identification of potential SPP homologs may in fact expand the number of potential proteases, which may account for γ-secretase activity in systems that exclude the action of presenilins (*20*). Identification of functional human SPP may allow elucidation of the mechanism of intramembrane proteolysis and address the still-unsolved question of how the cleavage of peptide bonds can be achieved in an environment that is thought to preclude hydrolysis.

**References and Notes**


1. M. S. Brown, J. Ye, R. B. Rawson, J. L. Goldstein, *Cell* **100**, 391 (2000).
2. K. Haze, H. Yoshida, H. Yanagi, T. Yura, K. Mori, *Mol. Biol. Cell* **10**, 3787 (1999).
3. Y. M. Chan, Y. N. Jan, *Neuron* **23**, 201 (1999).
4. J. R. Lee, S. Urban, C. F. Garvey, M. Freeman, *Cell* **107**, 161 (2001).
5. D. J. Selkoe, *Nature* **399**, A23 (1999).
6. H. Steiner, C. Haass, *Nature Rev. Mol. Cell Biol.* **1**, 217 (2000).
7. A. Weihofen, M. K. Lemberg, H. L. Ploegh, M. Bogyo, B. Martoglio, *J. Biol. Chem.* **275**, 30951 (2000).
8. B. Martoglio, B. Dobberstein, *Trends Cell Biol.* **8**, 410 (1998).
9. M. K. Lemberg, F. A. Bland, A. Weihofen, V. M. Braud, B. Martoglio, *J. Immunol.* **167**, 6441 (2001).
10. V. M. Braud *et al.*, *Nature* **391**, 795 (1998).
11. J. McLauchlan, M. K. Lemberg, R. G. Hope, B. Martoglio, in preparation.
12. J. Brunner, *Methods Enzymol.* **172**, 628 (1989).
13. Materials and methods are available as supporting material on *Science* online at www.sciencemag.org/cgi/content/full/296/5576/2215/DC1.
14. Single-letter abbreviations for the amino acid residues are as follows: A, Ala; C, Cys; D, Asp; E, Glu; F, Phe; G, Gly; H, His; I, Ile; K, Lys; L, Leu; M, Met; N, Asn; P, Pro; Q, Gln; R, Arg; S, Ser; T, Thr; V, Val; W, Trp; and Y, Tyr. X, any amino acid; h, hydrophobic amino acid.
15. M. S. Wolfe *et al.*, *Nature* **398**, 513 (1999).
16. H. Steiner *et al.*, *Nature Cell Biol.* **2**, 848 (2000).
17. S. Huppert, R. Kopan, *Dev. Cell* **1**, 590 (2001).
18. M. Szelke, in *Aspartic Proteinases and Their Inhibitors*, V. Kostka, Ed. (Walter de Gruyter, Berlin, 1985), pp. 421–441.
19. S. Moller, M. D. Croning, R. Apweiler, *Bioinformatics* **17**, 646 (2001).
20. S. S. Sisodia, W. Annaert, S. H. Kim, B. De Strooper, *Trends Neurosci.* **24**, S2 (2001).



21. We thank J. Brunner, B. Dobberstein, A. Helenius, and J. McLauchlan for discussions; C. Jakob for p426gal; and U. Kutay for the cDNA library. Supported by grants from Natural Sciences and Engineering Research Council of Canada Industrial Postgraduate Scholarship with MDS Sciex (K.B.), Eidgenössische Technische Hochschule Zürich, the National Competence Center for Research on Neuronal Plasticity and Repair, and the Swiss National Science Foundation (B.M.).

15 February 2002; accepted 11 April 2002


# Visualization and Functional Analysis of RNA-Dependent RNA Polymerase Lattices


**John M. Lyle,[1]* Esther Bullitt,[2]* Kurt Bienz,[3] Karla Kirkegaard[1]†**



**Positive-strand RNA viruses such as poliovirus replicate their genomes on intracellular membranes of their eukaryotic hosts. Electron microscopy has revealed that purified poliovirus RNA-dependent RNA polymerase forms planar and tubular oligomeric arrays. The structural integrity of these arrays correlates with cooperative RNA binding and RNA elongation and is sensitive to mutations that disrupt intermolecular contacts predicted by the polymerase structure. Membranous vesicles isolated from poliovirus-infected cells contain structures consistent with the presence of two-dimensional polymerase arrays on their surfaces during infection. Therefore, host cytoplasmic membranes may function as physical foundations for two-dimensional polymerase arrays, conferring the advantages of surface catalysis to viral RNA replication.**


Nucleic acid synthesis is often associated with large, static "factories" (*1*). For positive-strand RNA viruses such as poliovirus, foot-and-mouth disease virus, hepatitis C virus, and many others, the RNA replication complexes form on the cytosolic surface of cytoplasmic membranes (*2–4*). The role of this membrane association is not known, but it may be to (i) concentrate and compartmentalize viral products by targeting to a common structure, (ii) provide key lipid constituents to the viral RNA replication complexes, or (iii) physically support the RNA replication complex.

Poliovirus RNA synthesis is catalyzed by a virally encoded RNA-dependent RNA polymerase, termed 3D (*5*). The 3D polymerase is a soluble enzyme, but it is targeted to membranes by binding to another viral protein, 3AB (*6–8*), also part of the RNA replication complex. Poliovirus polymerase forms homo-oligomers, as demonstrated by its cooperative elongation and RNA-binding activity with respect to protein concentration, facile cross-linking with glutaraldehyde (*9*, *10*), and interactions in a yeast two-hybrid system (*7*, *11*). The three-dimensional crystal structure of the poliovirus polymerase determined by x-ray crystallography (*12*) revealed two interfaces between polymerase molecules (Fig. 1A). Based on a right-hand metaphor for polymerase structure, Interface I involves residues on the side of the thumb domain and residues on the back of the palm of an adjacent polymerase, forming a head-to-tail oligomeric fiber through the crystal (*12*). Amino acid substitutions predicted to disrupt interface I are lethal to the virus (*13*, *14*) and reduce RNA-binding affinity (*14*). Interface II involves intermolecular donation of the $NH_2$-terminal domain of one polymerase to a region of the thumb near the active site of its neighboring polymerase, forming a head-to-tail fiber through the crystal that intersects the fibers formed by interface I at a 90° angle (Fig. 1A) (*12*). However, the region of 3D polymerase around interface II is not completely resolved in the x-ray structure (*12*), and alternative crystal forms reveal that alternative packing conformations around interface II allow polymerase-polymerase interactions in this region, even in the absence of the $NH_2$-terminal donation (*15*). For wild-type polymerase, the existence of the intermolecular $NH_2$-terminal donation shown


[1]Department of Microbiology and Immunology, Stanford University School of Medicine, Stanford, CA 94305, USA. [2]Department of Physiology and Biophysics, Boston University School of Medicine, Boston, MA 02118, USA. [3]Institute for Medical Microbiology, University of Basel, CH-4003 Basel, Switzerland.

*These authors contributed equally to this work.
†To whom correspondence should be addressed. E-mail: karlak@leland.stanford.edu

in Fig. 1A has been substantiated by intermolecular cross-linking of engineered cysteine residues (*14*). The abrogation of polymerase activity and viral viability by mutations in the $NH_2$-terminal region shows that the $NH_2$-terminal sequences, and likely their intermolecular donation, are essential for polymerase function (*14*). In combination, biochemical, mutational, and structural data suggest that the oligomeric association of polymerase through interfaces I and II is required for RNA replication in infected cells.

To investigate the higher-order structure of poliovirus 3D polymerase, we evaluated electron micrographs of purified enzymes. Wild-type polymerase, purified to 99% homogeneity, formed large sheets—planar arrays hundreds of polymerase molecules in length and width (Fig. 1B). These two-dimensional lattices of polymerase can also take the form of twisted sheets and tubes, with diameters ranging from 400 to 1000 Å (Fig. 1C, "t") so that at least 20 polymerases compose their circumference. Electron-dense regions 60 Å thick along the edges of the polymerase tubes (Fig. 1C, arrowhead) indicate that the tubes are one polymerase thick. Upon prolonged incubation at 4°C, fibers ("f") with a diameter of 120 Å (two polymerases) extended from the ends of tubes and sheets (Fig. 1C).

We determined the effects of two sets of mutations on the higher-order structures observed by electron microscopy. The ΔIntI mutant polymerase R455A:R456A:L446N ($Arg^{455}$→Ala:$Arg^{456}$→Ala:$Leu^{446}$→Asn) is predicted to disrupt intermolecular interface I (Fig. 1A). ΔIntI polymerases formed only fibers 120 Å in width, similar to those seen with prolonged incubation of wild-type polymerase (Fig. 1D). This is in marked contrast to the predominant species of large sheets and tubes seen with wild-type polymerase.

The Δ65 mutant polymerase, lacking the $NH_2$-terminal 65 amino acids, is predicted to disrupt interface II, although the extent of disruption is unknown because the precise disposition of the $NH_2$-terminal strand in interface II differs among three different polymerase crystal forms (*15*). Electron microscopy (Fig. 1E) revealed that the mutant polymerase retained the ability to form large, ordered sheets and tubes. However, wild-type and Δ65 polymerases (Fig. 1, C and E) revealed differences in the diameters of the tubes formed and in the lattice parameters, as determined by visual inspection and by Fourier transform analysis (*16*). Polymerases that carry mutations designed to alter Interface I and II, containing both the ΔIntI and Δ65 mutations, did not form ordered structures (*16*). Therefore, the integrity of both interfaces I and II contributes to formation of the oligomeric structures of wild-type polymerase shown in Fig. 1.

Electron microscopic images do not necessarily reflect the majority of molecules in a population. To test whether a large proportion of the polymerase molecules in solution could oligomerize into large structures, we performed turbidity assays as described (*17*). Polymerase showed a marked increase in turbidity upon incubation; this increased turbidity was dependent on the presence of the interfaces seen in the crystal structure (Fig. 1F).

We examined the ability of mutant polymerases to function in RNA binding and in RNA elongation. We performed RNA binding and polymerization assays with heteropolymeric RNA HP1 (Fig. 2A) as a substrate for the polymerase. RNA HP1 is a 110-nucleotide (nt) RNA derived from the 3' noncoding region of poliovirus RNA, which

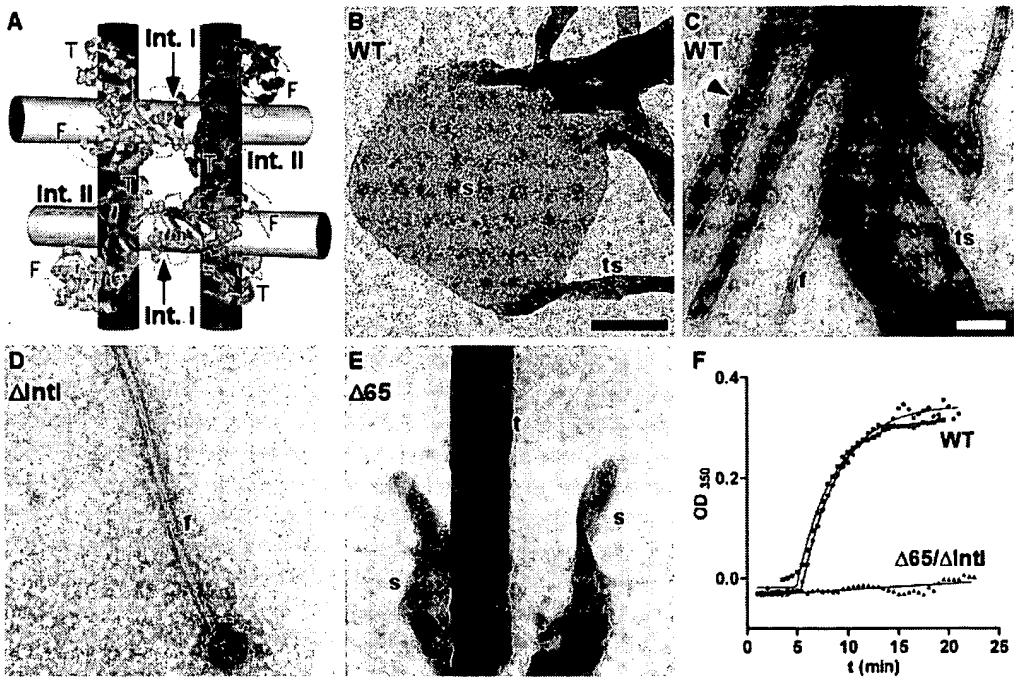


**Fig. 1.** Mutations that disrupt polymerase-polymerase interactions at interface I and interface II disrupt higher-order polymerase structures. (**A**) Crystallographic unit cell of the three-dimensional structure of poliovirus RNA-dependent RNA polymerase. Two sets of intermolecular contacts, interface I and interface II, are indicated (*12*). The four polymerase monomers that compose the unit cell are shown in different colors, with the thumb (T) and finger (F) domains indicated. The orientation of the polymerase fibers in the published three-dimensional structure is shown by the lattice posts and predicts an unlimited three-dimensional array. The wild-type amino acids, which are mutated in the ΔIntI polymerase (R455A:R456A:L446N), are shown as space-filling representations. The resolved portions of the $NH_2$-terminal 65 amino acids, deleted in the Δ65 mutation as a partial disruption of interface II, are seen in the thumb region in the color of the adjacent molecule from which they originate. Molecular modeling was performed with the Swiss PDB Viewer and rendered with POV-RAY (*37*). Coordinates for the unit cell of the three-dimensional structure of poliovirus RNA-dependent RNA polymerase were provided by J. Hansen (Yale University) and S. Schultz (Diné College) and can be obtained from the National Center for Biotechnology Information library under PDB identification number 1RDR. Cloning, mutagenesis, and purification methods were as described (*38*). (**B** to **E**) Images of nega-tively stained preparations of purified polymerase. Bars, 1000 Å. Magnifications in (C), (D), and (E) are identical. (B and C) Sheets (s), tubes (t), fibers (f), and twisted sheets (ts) formed by wild-type (WT) poliovirus polymerase. The arrowhead in (C) indicates the edge of a tube, with a wall thickness of ~60 Å. (D) A 120 Å fiber formed by ΔIntI polymerase. (E) Sheets and tubes formed by Δ65 polymerase. Polymerase was present in these reactions at 2 μM. (**F**) Optical density at 350 nm of 15 μM polymerase upon dilution into 10 mM tris-HCl (pH 7.5), 40 mM NaCl, and 30% glycerol with incubation at 25°C. Two independent time courses with wild-type (WT) polymerase and one time course with a polymerase containing both the Δ65 and ΔIntI mutations are shown.

includes 20 nt of polyadenylate and 5 U residues designed to form a self-priming RNA hairpin structure (*9*). As was seen for smaller substrates, disruption of interface I, but not interface II, reduced polymerase affinity for RNA (Fig. 2B) (*14*). Polymerase that contained both the Δ65 and the ΔIntI mutations showed RNA-binding affinity similar to that of polymerase that contained only the ΔIntI mutation (Fig. 2B). Therefore, the integrity of interface I, but not interface II, is required for high-affinity RNA binding.

The ability of wild-type and mutant polymerases to elongate RNA HP1 varied significantly. No elongation activity was observed for polymerase with disrupted interface II (*16*), corroborating previous reports that polymerase activity is sensitive to $NH_2$-terminal mutations (*14*, *18*). At pH 7.5, both wild-type and ΔIntI polymerase were capable of elongating RNA HP1, although ΔIntI polymerase was less efficient (Fig. 2C). At this pH, formation of the oligomeric sheets in solution (Fig. 1) required long incubation periods, and oligomerization was not cooperative with respect to concentration. At pH 5.5, a condition under which polymerase oligomerization occurs rapidly (*9*, *16*), polymerase activity is optimized and elongation of RNA HP1 is highly cooperative (Fig. 2D) (*9*). Under these conditions, ΔIntI mutations substantially reduced the cooperativity of RNA HP1 elongation (Fig. 2D). Therefore, the elongation activity at pH 7.5 (Fig. 2C) does not reflect the activity of highly oligomerized polymerase, and little effect of the ΔIntI mutations was observed. The low pH optimum for poliovirus polymerase activity and oligomerization could reflect the lack of protein and membrane cofactors that normally increase the rate of oligomerization, or it could reflect the actual pH on the surface of the membranes in infected cells. Although derived from the endoplasmic reticulum (*19*, *20*), the membranes on which poliovirus

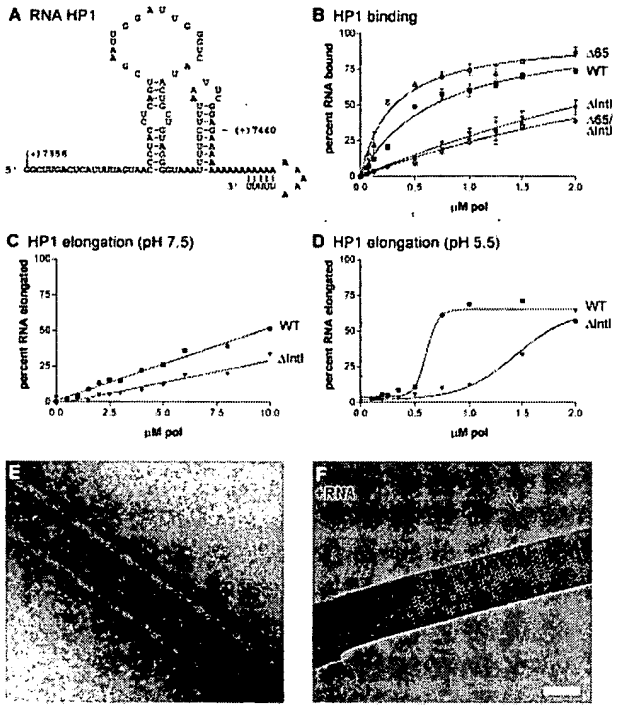


**Fig. 2.** Effect of mutations at interfaces I and II on polymerase binding and template utilization of 110-nt RNA. (**A**) Predicted secondary structure of the 110-nt RNA HP1 (*9*) used as a binding substrate and elongation template. The amount of total RNA HP1 bound in the presence of increasing polymerase concentration was measured by a nitrocellulose filter assay as described (*5*) and is plotted for wild-type (WT) (■), ΔIntI polymerase (▼), Δ65 (ΔΔ), and ΔIntIΔ65 (◇) polymerases at pH 7.5 (**B**). The extent of elongation of $^{32}$P-labeled HP1 RNA under these conditions is shown as a function of polymerase concentration for wild-type (■) and ΔIntI (▼) polymerases at pH 7.5 (**C**) and pH 5.5 (**D**). Negatively stained preparations of wild-type polymerase at 2 μM are shown in the absence (**E**) and presence (**F**) of 4 μM oligo(U)$_{24}$.

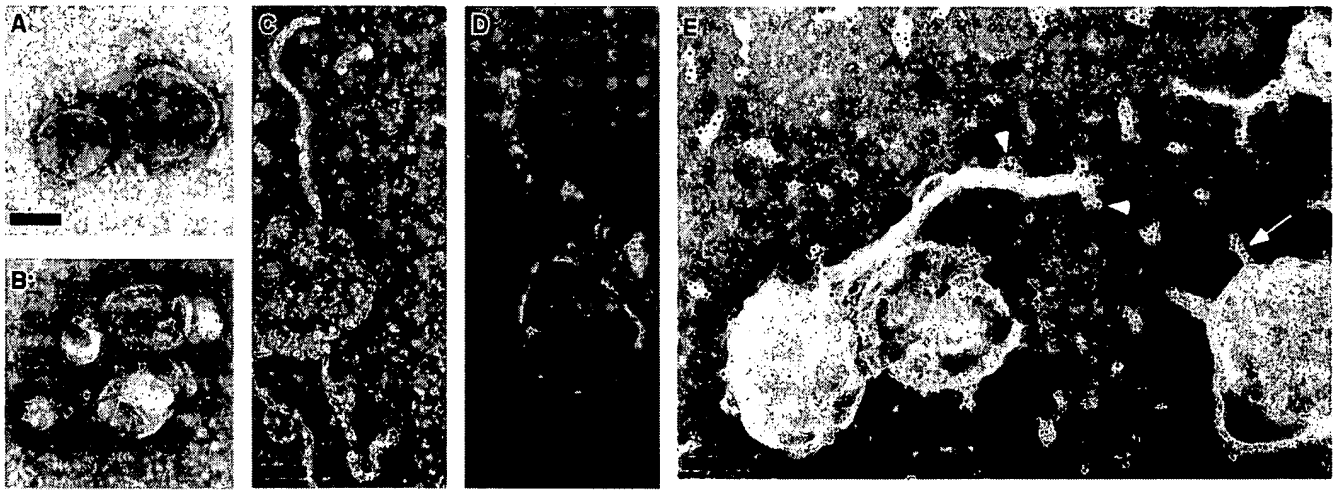


**Fig. 3.** Electron micrographs and immunostaining of membranous vesicles induced during poliovirus infection. Images of negatively stained preparations of membranous vesicles, isolated from poliovirus-infected HeLa cells as described (*25*), are shown. Poliovirus infections were performed in the absence (**A**, **C**, and **E**) or presence (**B** and **D**) of nocodazole (10 μg/ml) and cytochalasin (5 μg/ml) to test the role of the cytoskeleton in the formation of tubular structures. The effectiveness of this treatment was shown by vesiculation of the Golgi (staining with [(7-nitro-2-1,3-benzoxadiazol-4-yl)amino]dodecanoyl-ceramide; Molecular Probes) (*16*) and loss of integrity of actin filaments [staining with rhodamine-conjugated phalloidin; Molecular Probes (*16*)]. Electron micrographs of isolated vesicles from cells infected with poliovirus in the absence (A) orpresence (B) of nocodazole and cytochalasin with mouse monoclonal antibody to polymerase followed by goat antibody to mouse IgG coupled to 100 Å gold beads in the presence of 160 mM NaCl. Isolated vesicles are shown from cells infected with poliovirus in the absence (C) or presence (D) of nocodazole and cytochalasin that were incubated in a solution containing 30 mM NaCl before staining. Immunostaining of such vesicles with mouse monoclonal antibody to polymerase followed by goat antibody to mouse IgG coupled to 50 Å gold beads is shown (E). Arrow indicates 120 Å filament, and arrowheads indicate staining at the end and at a disruption in the larger (200 to 400 Å) tubes. Bars, 1000 Å. Magnifications in (A) and (B) and in (C) and (D) are identical.

RNA replication occurs also contain lysosomal markers (*21*), and the local pH in the RNA replication complexes is not known.

That the large oligomeric polymerase lattices themselves are RNA-binding structures can be seen from the marked increase in ordering of lattices formed in the presence of RNA (Fig. 2, E and F). Nonetheless, the formation of large two-dimensional sheets and tubes by purified polymerase in solution does not address whether such structures form in infected cells. Indeed, the presence of 400 to 1000 Å tubes has not been reported in intact cells, despite many descriptions of the ultrastructure of poliovirus-infected cells [for example, (*19–24*)]. However, Egger *et al.* (*25*) described the formation of tubules emanating from preparations of membranous vesicles obtained from poliovirus-infected cells after centrifugation and incubation in low-salt solutions. These membranous vesicles were shown to contain all viral proteins required for RNA replication (*25*).

We have investigated the structure of these tubules. Tubules from poliovirus-induced vesicles were formed as described (*25*) from cells treated with nocodazole and cytochalasin D (Fig. 3A). These drugs, which target microtubules and microfilaments, respectively, disrupt all cellular cytoskeletal elements, including intermediate filaments, which are dependent on the presence of intact microtubules and microfilaments for their integrity (*26*) but have no effect on the replication of poliovirus, suggesting that an intact cytoskeleton is not required for formation of the RNA replication complex (*27*). Poliovirus infection produced vesicles with viral polymerase on their surface in both treated and untreated cells (Fig. 3, A and B). Upon incubation in low-salt solution, tubular structures extruded from membranous vesicles in both cases (Fig. 3, C and D), indicating that these structures did not require the integrity of the cellular cytoskeleton.

Immunostaining showed that polymerase was present on fibers of ~120 Å diameter and on detached aggregates. Thus, under conditions similar to those that induce tube formation in vitro, polymerase was found on tubular protrusions resembling those found in purified enzyme preparations. Therefore, we suggest that tubule formation from the poliovirus-induced membranes under low-salt conditions is indicative of the presence of sheets of polymerase coating the membranes in poliovirus-infected cells. Larger tubules stained for polymerase only at ends or at structural distortions (Fig. 3E), making it likely that they contain other components in addition to polymerase. A possible scenario is that these tubules consist of a core of polymerase that was initially present on the membrane surface and, upon extrusion, remained attached to other components of the RNA replication machinery. Such structures also contain other viral replication proteins such as 2C and 2BC (*25*).

Although it was thought that poliovirus polymerase functions as an oligomer (*9*, *10*, *12*, *13*, *28*) and two sets of intermolecular contacts were revealed in the unit cell of the three-dimensional structure (*12*), the large assemblies seen by electron microscopy were unexpected (Fig. 1). For wild-type polymerase, these large, ordered arrays are often seen as flat sheets. These lattices also take the form of tubes of various diameters. The formation of these large assemblies appears to be a critical component in high-affinity RNA binding and, therefore, in RNA elongation.

Other proteins have been shown, in isolation, to form two-dimensional lattices. Interconversion between flat sheets and tubular structures is seen at the polymerizing end of eukaryotic microtubules (*29*), and such interconversions may also be important in the polymerization of FtsZ, a protein found in the septal plate during bacterial cell division (*30*). Protein p1 of bacteriophage ϕ29 is postulated to mediate the association of the phage DNA replication complex with host cell membranes and, in isolation, forms large protofilament sheets (*31*). For poliovirus polymerase, we hypothesize that the formation of two-dimensional sheets (Fig. 1B) by purified polymerase reflects the functional oligomerization of the polymerase into large lattices that coat the membranes upon which poliovirus RNA replicates in infected cells. The use of a planar membrane surface for nucleic acid replication complexes in such diverse systems as positive-strand RNA viruses, ϕ29 DNA phage, and bacterial genome replication (*32*, *33*) may indicate that this strategy is of broad use in diverse biological systems.

In contrast to ϕ29 p1 protein, poliovirus polymerase is not itself a membrane-associated protein. However, it binds specifically to another viral protein, 3AB, which associates with intracellular membranes. We previously identified a specific surface on the polymerase molecule for 3AB binding, consisting of polymerase residues $Phe^{377}$, $Arg^{379}$, $Glu^{382}$, and $Val^{391}$ (*7*, *8*). Figure 4 presents a model in which polymerase molecules are shown interacting along interface I in the horizontal direction. The polymerases are attached to the membrane through their interaction with 3AB molecules. Because each polymerase in these fibers is rotated 180° with respect to the adjacent polymerase (*12*), the 3AB-interacting surface could contact the membrane every second polymerase molecule. It is likely that this tethering of polymerase to membranes increases its local concentration, facilitating oligomerization into structures such as that shown in Fig. 1B.

Our data suggest that RNA replication occurs on a catalytic shell of polymerase molecules. We suggest that such two-dimensional lattices of enzyme are analogous to surface catalysts. Advantages of surface catalysis include a reduction in dimensionality of collisions between reactants, an increase in substrate affinity that can result from the clustering of multiple binding sites (*34*), and retention of the products of sequential reactions (*35*). Retention of products is particularly relevant to the genome replication of RNA viruses, because the negative-strand product serves as a template for a positive strand to complete a round of repli-

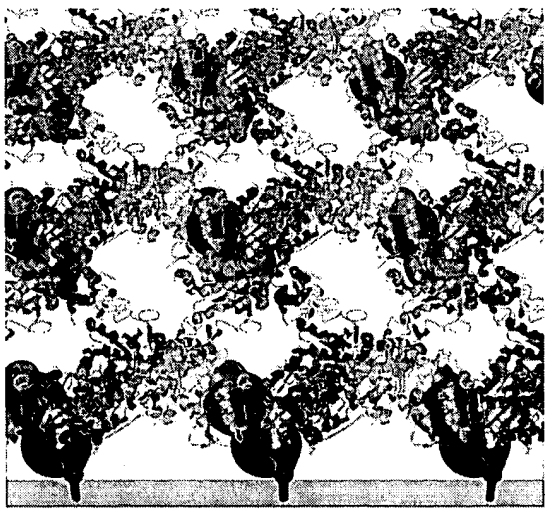

**Fig. 4.** Model of higher-order polymerase structure during poliovirus infection. One model for polymerase array formation is shown. To model this structure on intracellular membranes, we altered the angle of interaction of fibers interacting at interface II to allow for the formation of a planar lattice. Flexibility is more likely around interface II than around interface I, given the variability of interface II between different crystal forms of the polymerase (*15*). 3AB is represented as a globular, integral membrane protein in black (3a) and gray (3b); the dimerization of 3AB is the simplest interpretation of 3A-3A interactions observed in a two-hybrid system (*11*). Fibers of polymerase connected along interface I lie horizontally. These fibers are connected to one another through interactions at interface II, modeled to extend the lattice as a planar array, shown in perspective. Contacts with 3AB through the 3AB binding site (*7*, *8*), rendered in space-filled yellow side chains, could occur at every other polymerase along the axes defined by both interfaces. The figure was constructed and rendered as described in Fig. 1.

cation. The presence of multiple binding sites results in a high avidity of the polymerase array for single-stranded RNA, retaining the intermediates of RNA amplification while maintaining a low local affinity at each polymerase to allow the local template and primer movements necessary for processive RNA elongation. RNA recombination, which occurs by template switching during RNA replication (*36*), is responsible for much of the diversity of RNA viruses. The high frequency of switching between RNA templates might result from the presence of multiple templates and nascent strands on a shared polymerase lattice.


**References and Notes**

1. P. R. Cook, *Science* **284**, 1790 (1999).
2. E. Wimmer, C. U. T. Hellen, X. Cao, *Annu. Rev. Genet.* **27**, 353 (1993).
3. J. H. Strauss, E. G. Strauss, *Microbiol. Rev.* **58**, 491 (1994).
4. T. J. Chambers, C. S. Hahn, R. Galler, C. M. Rice, *Annu. Rev. Microbiol.* **44**, 649 (1990).
5. T. A. Van Dyke, J. B. Flanegan, *J. Virol.* **35**, 732 (1980).
6. J. Lama, A. V. Paul, K. S. Harris, E. Wimmer, *J. Biol. Chem.* **269**, 66 (1994).
7. D. A. Hope, S. E. Diamond, K. Kirkegaard, *J. Virol.* **71**, 9490 (1997).
8. J. M. Lyle *et al.*, *J. Biol Chem.* **277**, 16324 (2002).
9. J. Pata, S. C. Schultz, K. Kirkegaard, *RNA* **1**, 466 (1995).
10. M. T. Beckman, K. Kirkegaard, *J. Biol. Chem.* **273**, 6724 (1998).
11. W. Xiang, A. Cuconati, D. Hope, K. Kirkegaard, E. Wimmer, *J. Virol.* **72**, 6732 (1998).
12. J. L. Hansen, A. M. Long, S. C. Schultz, *Structure* **5**, 1109 (1997).
13. S. E. Diamond, K. Kirkegaard, *J. Virol.* **68**, 863 (1994).
14. S. D. Hobson *et al.*, *EMBO J.* **20**, 1153 (2001).
15. S. D. Hobson, thesis, University of Colorado, Boulder (2000).
16. J. M. Lyle, E. Bullitt, K. Bienz, K. Kirkegaard, unpublished data.
17. H. Flyvbjerg, E. Jobs, S. Leibler, *Proc. Natl. Acad. Sci. U.S.A.* **93**, 5975 (1996).
18. S. J. Plotch, O. Palant, Y. Gluzman, *J. Virol.* **63**, 216 (1989).
19. D. A. Suhy, T. H. Giddings Jr., K. Kirkegaard, *J. Virol.* **74**, 8953 (2000).
20. R. C. Rust *et al.*, *J. Virol.* **75**, 9808 (2001).
21. A. Schlegel, T. H. Giddings Jr., M. S. Ladinsky, K. Kirkegaard, *J. Virol.* **70**, 6576 (1996).
22. S. Dales, H. J. Eggers, I. Tamm, G. E. Palade, *Virology* **26**, 379 (1965).
23. K. Bienz, D. Egger, L. Pasamontes, *Virology* **160**, 220 (1987).
24. K. Bienz, D. Egger, T. Pfister, M. Troxler, *J. Virol.* **66**, 2740 (1992).
25. D. Egger, L. Pasamontes, R. Bolten, V. Boyko, K. Bienz, *J. Virol.* **70**, 8675 (1996).
26. M. W. Klymkowsky, *Nature Cell Biol.* **1**, 121 (1999).
27. J. R. Doedens, L. A. Maynell, M. W. Klymkowski, K. Kirkegaard, *Arch. Virol.* **9**, 159 (1994).
28. A. V. Paul *et al.*, *Virology* **272**, 72 (2000).
29. D. Chretien, S. D. Fuller, E. Karsenti, *J. Cell Biol.* **129**, 1311 (1995).
30. J. Löwe, L. A. Amos, *EMBO J.* **18**, 2364 (1999).
31. A. Bravo, M. Salas, *EMBO J.* **17**, 6096 (1998).
32. S. Winston, N. Sueoka, *Proc. Natl. Acad. Sci. U.S.A.* **77**, 2834 (1980).
33. C. Weigel *et al.*, *Mol. Microbiol.* **34**, 53 (1999).
34. G. L. Nelsestuen, *Chem. Phys. Lipids* **101**, 37 (1999).
35. A. R. Hill Jr., C. Bohler, L. E. Orgel, *Origins Life Evol. Biosph.* **28**, 235 (1998).
36. T. C. Jarvis, K. Kirkegaard, *EMBO J.* **11**, 3135 (1992).
37. Swiss PDB Viewer is described in N. Guex, M. C. Peitsch, *Electrophoresis* **18**, 2714 (1997) and is available at www.expasy.ch/spdbv. POV-RAY is available at www.povray.org.
38. Materials and methods are available as supporting material on *Science* Online at www.sciencemag.org/cgi/content/full/296/5576/2218/DC1.


39. We thank S. M. Crowder, K. C. Garcia, D. Egger, I. R. Lehman, E. Mocarski Jr., and P. Sarnow for critical reading of the manuscript; D. Egger for experimental contributions; and S. Schultz and R. Striker for experimental suggestions. J.M.L. is recipient of a predoctoral fellowship from the Howard Hughes Medical Institute. Funded by the Hutchison Foundation for Translational Research, Eli Lilly, Inc., NIH grant AI-42119, and Swiss National Science Foundation grant 1-055397.98.

5 February 2002; accepted 13 May 2002


# Covariation of Synaptonemal Complex Length and Mammalian Meiotic Exchange Rates


**Audrey Lynn,[1]* Kara E. Koehler,[1]* LuAnn Judis,[1] Ernest R. Chan,[1] Jonathan P. Cherry,[1] Stuart Schwartz,[1,2] Allen Seftel,[3,4] Patricia A. Hunt,[1] Terry J. Hassold[1]†**



**Analysis of recombination between loci (linkage analysis) has been a cornerstone of human genetic research, enabling investigators to localize and, ultimately, identify genetic loci. However, despite these efforts little is known about patterns of meiotic exchange in human germ cells or the mechanisms that control these patterns. Using recently developed immunofluorescence methodology to examine exchanges in human spermatocytes, we have identified remarkable variation in the rate of recombination within and among individuals. Subsequent analyses indicate that, in humans and mice, this variation is linked to differences in the length of the synaptonemal complex. Thus, at least in mammals, a physical structure, the synaptonemal complex, reflects genetic rather than physical distance.**


Virtually all human genetic linkage studies have examined individual chromosomes or chromosome segments. Consequently, little is known about the overall number and location of meiotic exchanges in individual germ cells. Only one systematic linkage analysis of genome-wide levels of recombination in humans has been published. Broman and colleagues (*1*, *2*) analyzed the inheritance of short tandem repeat polymorphisms in eight of the CEPH (Centre d'Etude du Polymorphisme Humain) reference families, examining all detectable recombination events per meiosis. This approach provides a useful tool for studying human recombination but has at least two limitations. First, it requires well-characterized, three-generation (or deeper) families. Hence, without acquisition of additional families, analysis is effectively limited to the few hundred meioses available from the CEPH registry. Second, the approach relies on analysis of transmitted haploid products instead of cells undergoing meiosis; consequently, only one-half of all exchanges can be detected (for example, after a single exchange, only two of the four chromatids are recombinant).

Recent cytological studies suggest that, by using antibodies against the DNA mismatch repair protein MLH1 to analyze meiosis I spermatocytes and oocytes (*3*), it may be possible to overcome these limitations. Specifically, studies analyzing the localization of MLH1 foci on synaptonemal complexes (SCs) in mouse (*4*) and human (*5*) spermatocytes suggested that these foci identify the sites of meiotic exchanges. However, as these analyses were based on small numbers of cells—45 spermatocytes from three mice (*4*) and 46 spermatocytes from a single human (*5*)—it was not possible to examine intra- and interindividual variation, nor was it possible to determine whether recombination varied with intrinsic or extrinsic factors (for example, the age of the individual).

To address these issues directly, we analyzed pachytene-stage cells from 14 control males (Fig. 1, table S1) (*6*); first, we asked whether the number and location of MLH1 foci conformed to expectations for a molecule that marks the sites of exchange. Details of these initial analyses are provided in supporting online text. Briefly, observations on 1384 cells from the 14 individuals yielded an overall mean of 49.1 ± 4.8 foci per cell and a range of 34 to 66 foci per cell, which is remarkably similar to data from CEPH males (fig. S1); estimates of chromosome-specific and total autosomal male maps were consis-


[1]Department of Genetics, Case Western Reserve University, [2]The Center for Human Genetics, University Hospitals of Cleveland, [3]Department of Urology, Case Western Reserve University and University Hospitals of Cleveland, [4]Cleveland VA Medical Center, 10900 Euclid Avenue, Cleveland, OH 44106, USA.

*These authors contributed equally to this work.
†To whom correspondence should be addressed. E-mail: tjh6@po.cwru.edu